Multiphysics Based Numerical Study of Atmospheric Ice Accretion on a Full Scale Horizontal Axis Wind Turbine Blade

M. Virk[1,2]*, U. Mughal[2], Q. Hu[1], X. Jiang[1]

1. State Key Laboratory of Power Transmission Equipment & System Security, Chongqing University, China

2. Arctic Technology Research Team, Institute of Industrial Technology, University of Tromsø, Norway

ABSTRACT

Atmospheric icing on wind turbines have been recognized as a hindrance to the development of the wind power in cold regions, where uncertainty surrounding the effects of icing on energy production may prevent otherwise good wind resources from being utilized. This research paper is focused on to numerically simulate the rate and shape of atmospheric ice accretion on a full-scale horizontal axis wind turbine blade. Computational fluid dynamics based multiphase numerical analyses have been carried out where results showed a decrease in atmospheric ice growth rate along leading edge with the increase of blade profile size, both in terms of local ice mass and thickness. Streamlined ice shapes were observed near the blade root section, as compared to the blade tip section.

1. INTRODUCTION

Cold regions have good resources of wind energy, where wind turbine operation is linked with the uncertainty regarding its performance under icing conditions. The amount of wind energy lost due to icing is an area of large uncertainty and must be addressed properly to improve the performance of wind turbine in cold regions [1]. International energy agency (IEA) annex XIX: '*Wind energy in cold climates*', have specified that one of its objectives is to find the methods to better estimate the effects of ice accretion on energy production'. Depending on the ice mechanism, the atmospheric ice can be classified as: dry rime, wet glaze or mixed ice [2, 3]. Duncan et al [4] differentiated between rime and glaze ice and it was estimated that glaze ice caused larger problems than rime ice [5]. Meteorological parameters such as atmospheric temperature, wind speed, droplet size and liquid water content significantly effects the ice accretion on wind turbines.

Ice accumulation on wind turbine blade occurs due to impingement of super cooled water droplets. Most of these liquid water droplets freeze immediately upon impingement due to rapid heat dissipation leading to ice accretion. The location and intensity of water impingement can be numerically determined by solving the air-water multiphase flow in proximity of the blade. The shape of the accreted ice on wind turbines depends upon many variables such as its point of operation, geometry, relative wind velocity, temperature, droplet diameter and the liquid water content [6]. Since last, few decades' numerical

*Corresponding Author: muhammad.s.virk@uit.no

methods have begun to play a significant role in investigating the effects of ice accretion on structures in cold regions.

Different researchers have simulated the effects of ice accretion on wind turbine blade profiles [7-9], but very few have simulated the ice growth on a full scale wind turbine blade. Homola et. al. [10] and Virk et. al. [3] have simulated the effects of dry and wet ice accretion on wind turbine blade profiles and found that wind turbine blade profile sections with longer chord length are less effected by ice accretion, as longer chord blade profiles generally has a larger leading edge radius, therefore incoming super cooled water droplets mainly follow the stream line across these profile sections and do not collide with the blade surface [11]. The effect of ice accretion on the blade profile is generally an altered profile shape resulting in a reduced lift coefficient (C_l) and increased drag coefficient (C_d) [12]. Shin et al.[13] described that the aerodynamic characteristics of the blade profile due to ice accretion changes with atmospheric temperature and that the drag coefficient had a temperature dependence that is relatively constant through the rime ice region, increases with increasing the temperature and then drops sharply as higher temperature melts the horns and ice. The higher drag coefficients at intermediate temperatures corresponds to the horn shaped icing causing a larger aerodynamic disturbance than the more streamlined dry rime ice [5]. In this paper computational fluid dynamics based multiphase, 3D numerical analyses have been carried out on a full-scale large horizontal axis wind turbine blade to simulate and analyse the ice growth along wind turbine blade.

2. NUMERICAL MODEL

Multiphase numerical modeling of atmospheric ice accretion on wind turbines is a complex coupled process, which mainly involves the air flow simulation, water droplet behavior, boundary layer characteristics and iced surface thermodynamics involving the phase change. Figure 1 shows a schematic view of coupling of different processes involved in multiphase icing simulations.

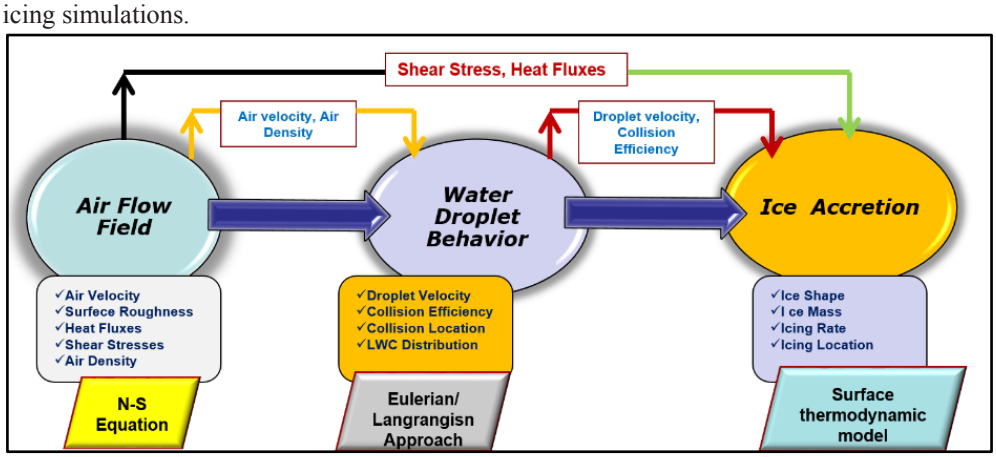

Figure 1: Schematic view of coupling of different processes involved in multiphase icing simulations.

For this research work, multiphase numerical analyses in this work were carried out using 'ANSYS FENSAP-ICE', where the airflow behavior is simulated by discretization of

governing PDE's for conservation of mass, momentum and energy. Continuity equation (Eq-1) was used for mass conservation, Navier Stokes equation (Eq-2) was used for the momentum conservation, whereas energy conservation was based upon first law of thermodynamics (Eq-3).

$$\frac{\partial \rho_a}{\partial t} + \nabla.\left(\rho_a.\vec{V}_a\right) = 0 \tag{1}$$

$$\frac{\partial \rho_a \vec{V}_a}{\partial t} + \vec{\nabla}.\left(\rho_a \vec{V}_a \vec{V}_a\right) = -\vec{\nabla}.\sigma^{ij} + \rho_a \vec{g} \tag{2}$$

$$\frac{\partial \rho_a E_a}{\partial t} + \vec{\nabla}.\left(\rho_a \vec{V}_a H_a\right) = \vec{\nabla}.\left(k_a.(\vec{\nabla}T_a) + \upsilon_i \tau^{ij}\right) + \rho_a g.\vec{V}_a \tag{3}$$

Where ρ_a is the air density, V_a is the air velocity, T_a is the air temperature, E_a is the air enthalpy and τ is the shear stress. For droplet behavior, Eulerian two phase flow model was used, which consists of Navier-Stokes equation augmented by droplets continuity and momentum.

$$\frac{\partial \alpha}{\partial t} + \vec{\nabla}.\left(\alpha \vec{V}_d\right) = 0$$

$$\frac{\partial (\alpha \vec{V}_d)}{\partial t} + \vec{\nabla}.\left(\alpha \vec{V}_d.\vec{V}_d\right) = \frac{C_D \,\mathrm{Re}_d}{24K}\alpha\left(\vec{V}_a - \vec{V}_d\right) + \alpha\left(1 - \frac{\rho_a}{\rho_d}\right).\frac{1}{F^2_r}.\vec{g} \tag{4}$$

Where α is the liquid water content, C_D is the drag coefficient, K is the droplet inertial parameter, d is the droplet diameter, L is the characteristic length and F_r is the Froude number. Ice accretion on a solid surface involves heat and mass transfer, where contamination caused by impinging water droplets is modeled as thin film of liquid, running along the blade surface. Part of this film may freeze, evaporate or sublimate. The coupled air flow and droplets equations are solved in time, with ice accretion computed from the surface thermodynamic model described by Messinger [14]. The model is based on the thermodynamic equilibrium and involves different heat fluxes (Q).

Un-structured type numerical grid was used for blade surface and domain, whereas to accurately determine the boundary layer characteristics (shear stresses and heat fluxes), a y+ value less than 1 was used near the wall. Figure 2 shows the computational mesh used for this study. The roughness height for the iced blade profiles was calculated according to Shin et al.[15]. The two-phase flow was solved using Eulerian-Eulerian approach. The main advantage of using Eulerian-Eulerian approach is that, the same mesh can be used for multiphase flow calculations and ice geometry. One-equation Spalart–Allmaras turbulence model was used as a compromise between acceptable computational cost and the required

accuracy in simulating the turbulent flow. To study the rate and shape of atmospheric ice accretion, analyses were carried out for t = 10 minutes, where each time step was $\Delta t = 0.001$ sec. The numerical simulations of the icing shapes were carried out at the operating conditions specified in Table-1.

$$\rho_f \left[\frac{\partial h_f}{\partial t} + \nabla . \left(V_f h_f \right) \right] = V_\infty . LWC \beta - m^o_{evap} - m^o_{ice} \tag{5}$$

$$Q^o_{in} = Q^o_{out} \tag{6}$$

$$Q_{latent\ heat} + Q_{aerodynamic\ heat} + Q_{KE\ heat} = Q_{sublimative\ heat} + Q_{convective\ heat} + Q_{droplet,cooling\ heat}$$

$$Q_{aerodynamic,heating} = \frac{r h_c v^2_\alpha}{2C_p} \tag{7}$$

r = *Adiabatic recovery factor*, ($r = P_r^{1/2}$ *for laminar and* $r = P_r^{1/3}$ *for turbulent flow*)

$P_r = 0.72$

C_p = *Specific heat of air*, 1006 *J / kgK*

$$Q_{latent,heat} = (LWC.\beta.v_\alpha).\left[L_f + C_i (T_{air} - T_{surface}) \right] \tag{8}$$

C_i = *Specific heat of ice*

L_f = *Latent heat of fusion*

$$Q_{droplrt,kinetic,energy} = (LWC.\beta.v_\alpha)\frac{v^2_\alpha}{2} \tag{9}$$

$$Q_{convection} = h_c (T_{surface} - T_{air}) \tag{10}$$

$$Q_{sublimation} = \chi_s e_o (T_{surface} - T_{air}) \tag{11}$$

$$\chi_s = \frac{0.622 h_c L_s}{C_p P_t L_e^{0.66}}$$

e_o = 27.03

L_S = *Latent heat of sublimation.*

L_e = *Lewis number*, $1/P_r$

$$Q_{droplet,cooling} = \rho_a \beta v_\alpha C_{p,w} (T_{surface} - T_{air}) \tag{12}$$

$C_{p,w}$ = *Specific heat of water*, 4218 *J / kgK*

Table 1: Operating conditions used for the simulations.

Air flow velocity (m/sec)	10
Atmospheric temperature (°C)	-10
Droplet velocity (m/sec)	10
Liquid water content (g/m^3)	1
Droplet media volume diameter (μm)	70
Icing simulation time (min)	10

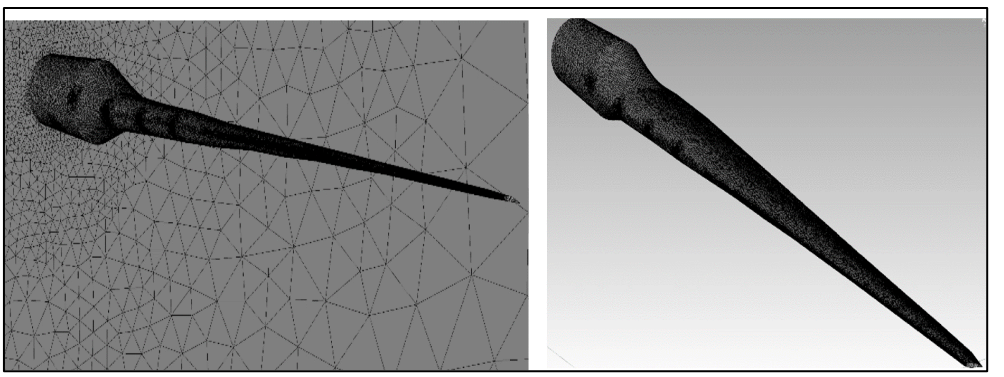

Figure 2: Computational mesh used for the study.

3. RESULTS & DISCUSSION

3.1 Flow Behaviour & Droplet Distribution

Numerical analyses of the airflow behaviour showed a change in the velocity and pressure distribution along wind turbine blade. Change of geometric characteristics along blade from tip to root leads to a change in the relative velocity and angle of attack that effectively changes the flow behaviour along each section. Such change in the blade geometric characteristics is generally to avoid the stall of the blade root section. High flow separation is observed near root section of the blade, as compared to the blade centre and tip. Figure 3 shows the free stream velocity vectors at v=10 m/s, across wind turbine blade.

Liquid water droplet moving in the air stream is generally influenced by its drag and inertia, when neglecting the gravity and buoyancy [16], If drag dominates the inertia, the droplet follows the stream line whereas for the case where inertia dominates the particle hits the object. The ratio of inertia to drag depends upon the droplet size, velocity of air stream and dimensions of the object in question. Therefore, with an increase in blade size (chord length) more droplets and especially the small droplets, move along the streamlines around the blade. As the wind turbine blade near the root have larger chord length and thickness, results show low droplet collision efficiency near the blade root section, while higher droplet collision efficiency is observed near the tip section. This trend is strengthened by changes in relative velocity. Lower relative velocity near the blade root reduces the influence of the inertial component of droplet motion and also allows more droplets to

follow the streamlines around the blade. Figure 4 shows the water droplet collision distribution along wind turbine blade.

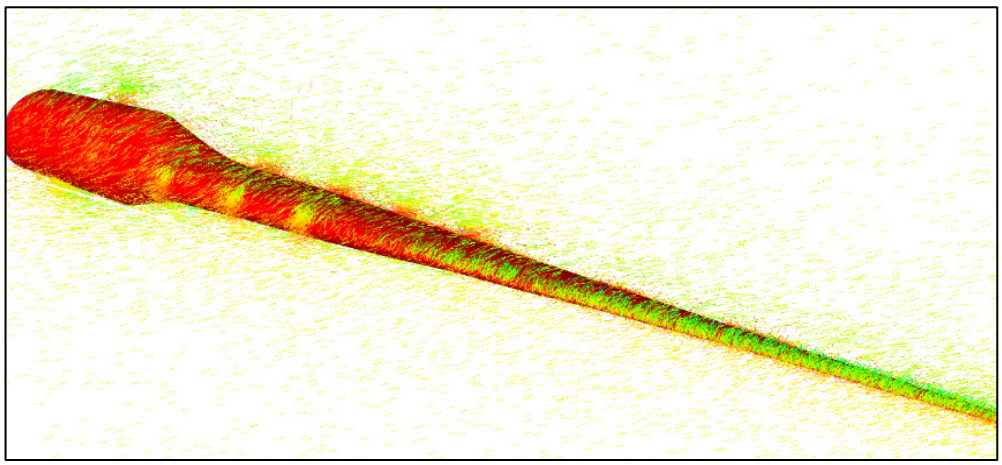

Figure 3: Free stream velocity vectors across wind turbine blade at v= 10 m/sec

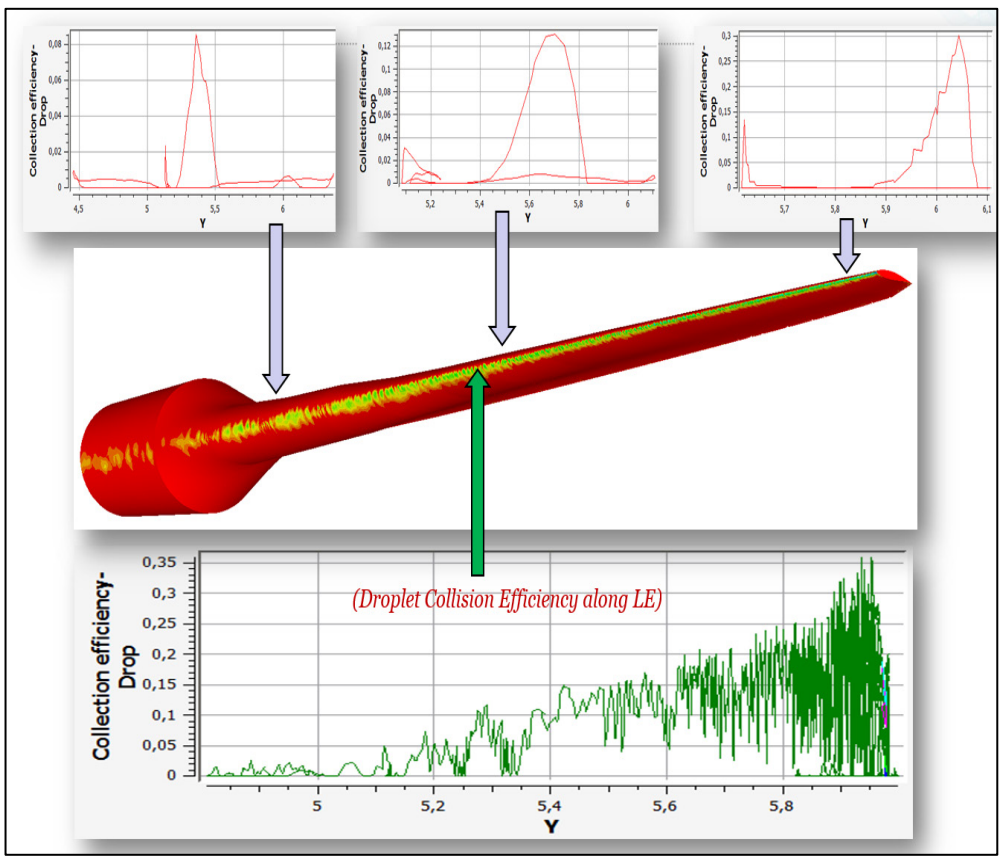

Figure 4: Water droplet collision along wind turbine blade

3.2 Atmospheric Ice Accretion

To study the rate and shape of ice accretion along the wind turbine blade, the numerical analyses were carried out for t = 10 minutes where each time step was $\Delta t = 0.001$ sec. Results show a decrease in ice accretion near the blade root as compared to the blade tip section. Such decrease is mainly due to the decrease in collision efficiency of the droplets with the blade surface and the reduction in velocity. Blade sections near tip has a smaller chord and blade thickness ratio, as well as a higher velocity, therefore more ice accretion was found at this section, whereas results show a gradual decrease in ice accretion, when moving towards the root of the blade. Figure 5 & 6 shows the atmospheric ice growth along wind turbine blade.

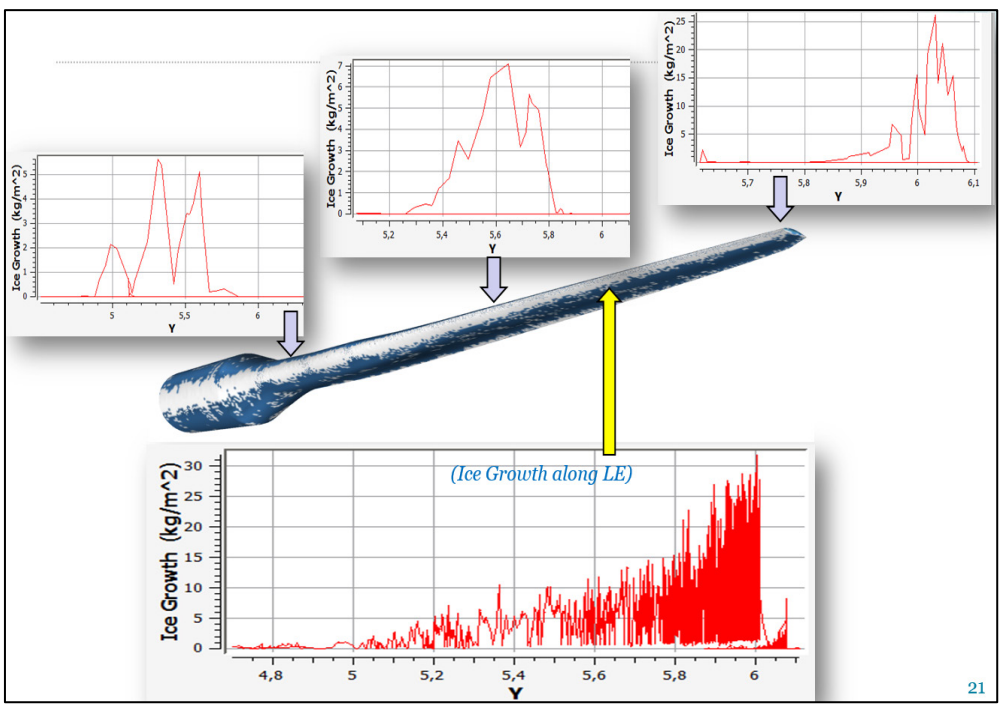

Figure 5: Atmospheric Ice growth rate along wind turbine blade.

In figure 5, a significant difference in ice growth can be seen from root to sections along the blade. Although the area covered by the ice near the root sections is larger, but the ice layer near the blade root is very thin, while near blade tip, the accreted ice is considerably thicker as compared to root. As mentioned above, with the increase of blade profile size from tip to root, the super cooled water droplets follow the stream line and their collision efficiency reduces which leads to decrease in rate of ice growth. As near the root, the blade has a larger chord and thickness therefore more water droplets follow the streamline and do not hit the blade surface, whereas near the blade tip, due to smaller profile size the collision efficiency of the droplet is high and more ice accretion is observed.

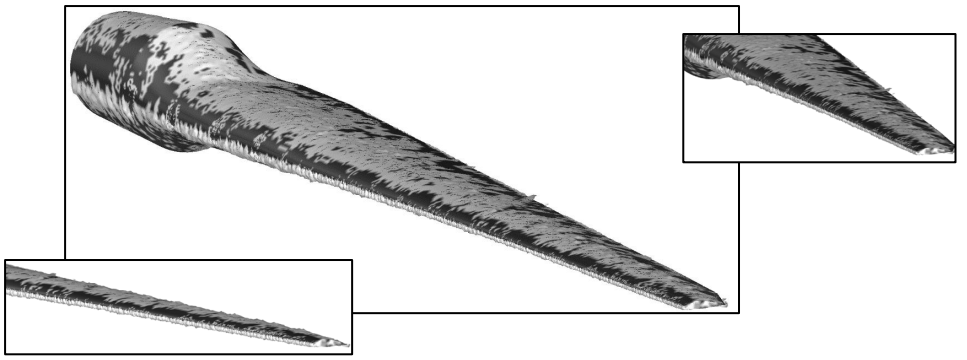

Figure 6: Atmospheric Ice accretion along wind turbine blade.

4. CONCLUSION

The rate and shape of ice accretion along a full-scale horizontal axis wind turbine blade is simulated using the CFD based multiphase numerical technique. The results indicate that the combined changes in blade profile size and relative velocity along the blade considerably influences the ice growth. Near the blade tip, where the blade chord length and thickness is less, more ice accretion was found as compared to the blade root. Overall, the results indicate that the icing is less severe for the blade sections, where the blade profiles are larger and thicker, both in terms of local ice mass and ice thickness. These numerical analyses show that there is a considerable change in the ice growth with the change in blade geometric parameters, which explores the possibility that by optimizing the blade geometric parameters the ice accretion on the wind turbine blades can be minimized, this means a passive anti/de-icing approach for wind turbine operations in cold regions.

ACKNOWLEDGEMENT

The work reported in this paper was supported by Visiting Scholarship of State Key Laboratory of Power Transmission Equipment & System Security and New Technology, (project number-2007DA10512714403), WindCoE (Nordic Wind Energy Centre) project funded within Interreg IVA Botnia-Atlantica, as part of European Territorial Cooperation (ETC) and Research Council of Norway, COLDTECH-RT 3, (project no. 195153).

REFERENCES:

[1] Matthew C Homola, et al., *Performance losses due to ice accretion for a 5 MW wind turbine.* Wind Energy, 2012. **15**(3): p. 379-389.

[2] Cao Y, Q Zhang, and J. Sheridan., *Numerical simulation of ice accretion on airfoils*, in *XXII ICTAM*. 2008: Adelaide, Australia.

[3] Muhammad S Virk, Matthew C Homola, and P.J. Nicklasson., *Effect of rime ice accretion on aerodynamic charactristics of wind turbine blade profiles.* Wind Engineering, 2010. **34**(2): p. 207-218.

[4] T Duncan, M Leblanc, and C. Morgan. *understanding icing losses and risk of ice throw at operating wind farms*. in *WinterWind*. 2008. Norrkoping, Sweden.

[5] Muhammad S Virk, Matthew C Homola, and p.J. Nicklasson., *Effect of atmospheric temperature and droplet size variation on ice accretion of wind turbine blades.* Wind engineering & industrial aerodynamics, 2010. **98**: p. 724-729.

[6] Peter, D. *Numerical simulation of ice accretion on wind turbines*. in *IWAIS 2009*. 2009.
[7] B Tammelin, et al. *Icing effects on power production of wind turbines*. in *BOREAS IV Conference*. 1998. Finish Meteorological Institute.
[8] M Marjaniemi and E. Peltola. *Blade heating element design and practical experiences*. in *BOREAS IV Conference*. 1998. Finish Meteorological Institute.
[9] M Marjaniemi, T Laakso, and L. Makkonen. *The wind turbine blade icing model*. in *BOREAS V Conference*. 2000. Finnish Meteorological Institute.
[10] Matthew C Homola, Per J Nicklasson, and P.a. sundsbø. *Experinces from icing at Nygårdsfjell wind park*. in *EWEC* 2008.
[11] C Bak, P Fuglsang, and N. Sørensen., *Airfoil charactristics for wind turbines*. 1999, Risø national loboratory.
[12] Holdo, A.E., et al., *Experimental simulation of runback ice.* Journal of aircraft, 1997. **34**: p. 206-212.
[13] J Shin, B Berkowitz, and H. Chen., *prediction of ice shapes and their effects on airfoil performance*. 1991: NASA Technical memorandum - 103701.
[14] L., M.B., *Equilibruim temperature of an unheated icing surface as a function of air speed.* journal of aeronautical sciences, 1953: p. 29-42.
[15] Shin J, et al., *Prediction of ice shapes and their effect on airfoil performance*. 1991, Technical Report, NASA Technical Memorandum 103701,.
[16] Mortensen, K., *CFD simulations of an airfoil with leading edge ice accretion*, in *Department of Mechanical Engineering*. 2008, Technical university of Denmark. p. 117.